Enantioselective Reductive Oligomerization of Carbon Dioxide into l -Erythrulose via a Chemoenzymatic Catalysis

Sarah Desmons, Katie Grayson-Steel, Nelson Nuñez-Dallos, Laure Vendier, John Hurtado, Pere Clapés, Régis Fauré, Claire Dumon, Sébastien Bontemps

Enantioselective reductive oligomerization of carbon dioxide into L-erythrulose via a chemo-enzymatic catalysis

Sarah Desmons,[*,†,‡] Katie Grayson-Steel,[‡] Nelson Nuñez-Dallos,[†,§] Laure Vendier,[†] John Hurtado,[§] Pere Clapés,[‖] Régis Fauré,[‡] Claire Dumon,[‡] Sébastien Bontemps[*,†]

[†] LCC-CNRS, Université de Toulouse, CNRS, F-31077 Toulouse Cedex 4, France

[‡] TBI, Université de Toulouse, CNRS, INRAE, INSA, 31077 Toulouse, France

[§] Department of Chemistry, Universidad de los Andes, Carrera 1 No. 18A-12, 111711, Bogotá, Colombia

[‖] Biological Chemistry Department, Instituto de Química Avanzada de Cataluña, IQAC-CSIC, Jordi Girona 18-26, 08034 Barcelona, Spain

ABSTRACT: Cell-free enantioselective transformation of the carbon atom of CO_2 has never been reported. In the urging context of transforming CO_2 into products of high value, enantiocontrolled synthesis of chiral compounds from CO_2 would be highly desirable. Using an original hybrid chemo-enzymatic catalytic process, we report herein the reductive oligomerization of CO_2 into C_3 (dihydroxyacetone, DHA) and C_4 (L-erythrulose) carbohydrates, with perfect enantioselectivity of the latter chiral product. This was achieved with the key intermediacy of formaldehyde. CO_2 is firstly reduced selectively by $4e^-$ with an iron-catalyzed hydroboration reaction leading to the isolation and complete characterization of a new bis(boryl)acetal compound derived from dimesitylborane. In an aqueous buffer solution at 30 °C, this compound readily releases formaldehyde which is then involved in selective enzymatic transformations giving rise either i) to DHA using a formolase (FLS) catalysis or ii) to L-erythrulose with a cascade reaction combining FLS and D-fructose-6-phosphate aldolase (FSA) A129S variant. Finally, the nature of the synthesized products is noteworthy since carbohydrates are of high interest for the chemical and pharmaceutical industries. The present results prove that cell-free *de novo* synthesis of carbohydrates from CO_2 as a sustainable carbon source, is a possible alternative pathway besides the intensively studied biomass extraction and *de novo* syntheses from fossil resources.

INTRODUCTION

Carbohydrates represent the most abundant class of biomolecules on Earth used as energy carrier, biomass building blocks and as key biologically active molecules, including antibiotics and anticancer agents.[1] The rich density of hydroxyl and carbonyl groups as well as of asymmetric carbon centers lead to a multiplicity of possible stereo- and regio-isomers. This large structural diversity allows them to encode information for specific molecular recognition processes, such as immune defense response, cell signaling and cell trafficking and to serve as determinants of protein folding, stability and pharmacokinetics.[2] As a consequence, carbohydrates - especially rare and non-natural sugars - are products of high value for the chemical and drug pharmaceutical industries.[3] Two main synthetic accesses are intensively being developed to synthesize these species: biomass extraction[4] and *de novo* syntheses from classical chemical feedstock derived from fossil resources.[3a, 5] While the most abundant carbohydrates are obtained from biomass extraction, the synthesis of rare or non-natural ones requires either i) further transformation from extracted abundant carbohydrates or ii) the use of *de novo* syntheses.[6]

Their generation from CO_2 would be a third complementary alternative offering *de novo* syntheses from a sustainable source of carbon. However, the improvement of the multi-enzymatic photosynthetic systems and notably of the Calvin-Benson-Bassham (CBB) cycle[7] for synthetic purposes in autotrophic[8] or heterotrophic[9] organisms still holds important challenges for targeting specific carbohydrate. In photosynthesis, the synthetic strategy can be summarized by the repetition of two elementary steps: i) carbon dioxide fixation followed by ii) reduction with NADPH and ATP (Scheme 1a), ultimately leading to the generation of glyceraldehyde-3-phosphate in the case of the CBB cycle.[10]

In absence of any bio-machinery, the generation of carbohydrates from CO_2 appears even more challenging despite the large body of research on CO_2 reduction.[11] It indeed implies the transformation of achiral triatomic and stable CO_2 molecules into complex products featuring a chiral poly-oxygenated carbon framework.[12] It also implies the use of CO_2 as a C_n source which is much less explored than as a C_1 source.[13] Moreover, cell-free enantioselective transformation of the carbon atom of CO_2 is unprecedented.[14] To achieve such challenging goal, we sought for a strategy differing from the natural photosynthetic strategy observed in the CBB cycle. We aimed at exploring the reduction of CO_2 into formaldehyde followed by a formose reaction corresponding to the oligomerization of formaldehyde into carbohydrates (Scheme 1a). Formaldehyde is a highly reactive and versatile molecule[15] and its oligomerization is arguably the most powerful transformation of this simple and achiral C_1 molecule.[16] As a consequence, the interest for the formose reaction spans different fields: from synthetic chemistry to space exploration and the search for the origin of life.[10, 17] The formation of carbohydrates from CO_2 via a formaldehyde-pathway was hypothesized with the observed formation of "reducible sugars" upon irradiating CO_2 at two different wavelengths in 1921[18] and to explain the formation of polyoxygenated compounds from the Ni-catalyzed electroreduction of CO_2 in 2018.[19]

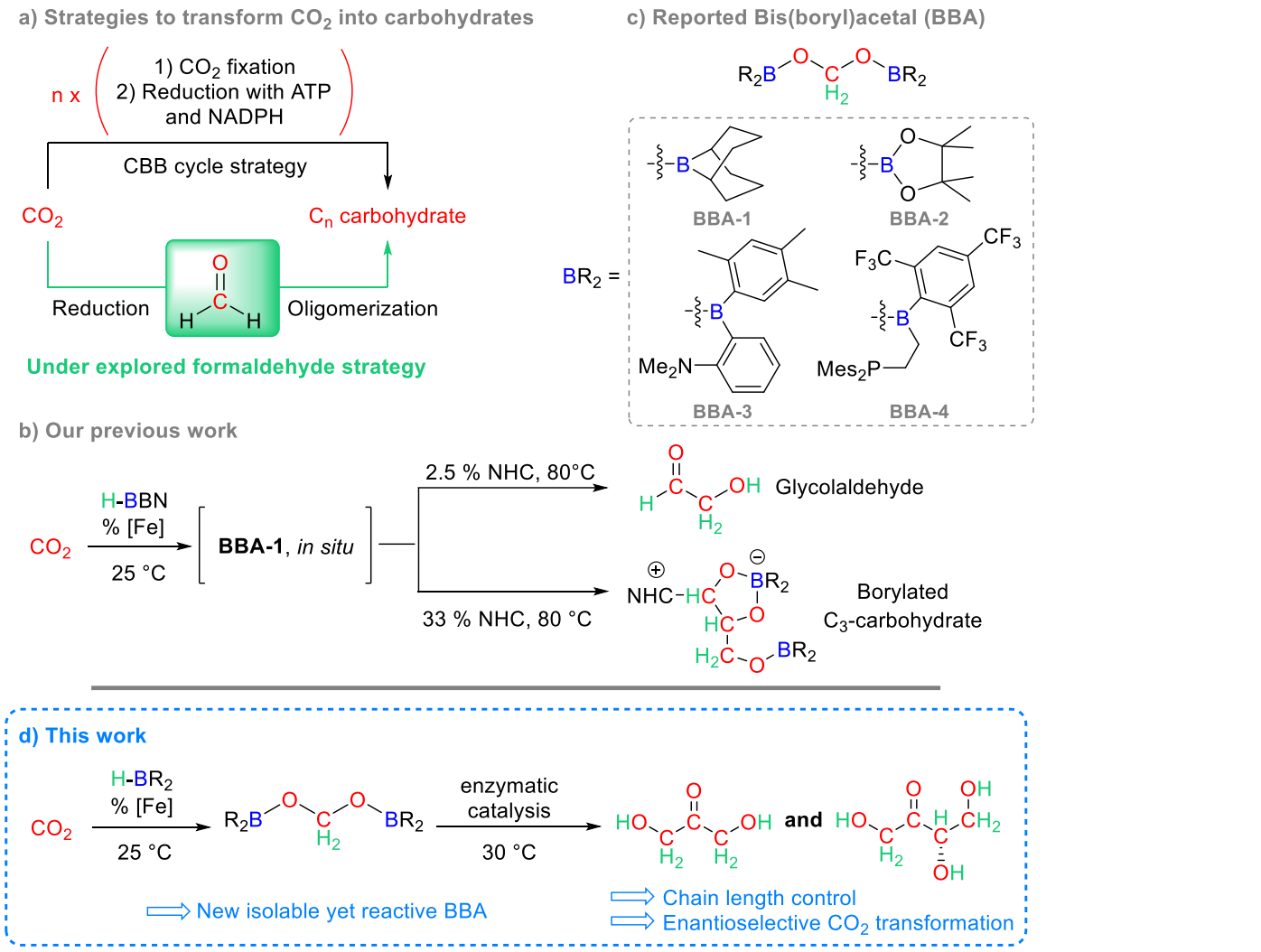

Scheme 1. a) CBB cycle and formaldehyde strategies for the transformation of CO_2 into carbohydrates, b) Our previous work, c) Reported bis(boryl)acetal obtained from CO_2 hydroboration reactions, d) Schematic view of the findings of the present publication

The intrinsic difficulty to conduct each step (*i.e.* 4e- reduction of CO_2 and HCHO oligomerization) and to associate two different catalytic processes certainly explain why such formaldehyde-strategy (Scheme 1a) has not been further explored for the synthesis of carbohydrates until our findings using *N*-heterocyclic carbene (NHC, Scheme 1b). We indeed recently reported the catalytic generation of glycolaldehyde (GA)[20] and the stoichiometric generation of a borylated C_3 carbohydrate[21] from CO_2 as the sole carbon source.

These findings were obtained with the intermediacy of a bis(boryl)acetal (BBA) compound featuring 9-borabicyclo[3.3.1]-nonane (9-BBN) moieties (**BBA-1**, Scheme 1c) resulting from the formal addition of 2 equiv. of 9-BBN on CO_2.[22] The reduction of CO_2 by hydroboranes was pioneered by Guan *et al.*[23] Adopting this reduction process,[24] we and others not only disclosed mechanistic understandings[25] but also controlled reduction, in particular to the 4e- reduction level.[22a, 26] So far, four BBA have been generated selectively (**BBA-1-4**, Scheme 1c). **BBA-1**[22a, 26] and **BBA-2**[27] were obtained from commercially available hydroboranes, 9-BBN and pinacolborane (HBpin), respectively, and their syntheses require the use of a catalyst. Both of them were found rather unstable in solution or under vacuum. Only **BBA-2** was recently isolated thanks to a particularly selective and efficient catalysis and taking advantage of its precipitation in the solvent medium.[27] **BBA-1** and **BBA-2** were both used as formaldehyde surrogates in C_1 transformation of CO_2.[22c, 27-28] In contrast, **BBA-3**[29] and **BBA-4**[30] were structurally characterized by X-Ray diffraction analysis and their syntheses do not require the use of a catalyst. In both cases, the presence of a pendant Lewis basic moiety is worth noticing and might explain why a catalyst was not necessary. To our knowledge, their reactivity in further transformation has not been reported. It is worth mentioning that in parallel to the C_1 chemistry of BBA, the synthesis and the C_1 chemistry of analogous bis(silyl)acetal compounds were also developed.[31]

As indicated above, we proved that **BBA-1** could also be used as a C_n source, but we stopped at glycolaldehyde (GA) - the smallest (C_2) and achiral carbohydrate - in the catalytic procedure.[20] We therefore hypothesized that enzymatic carbon-carbon bond formation would be instrumental for accessing longer-chain, higher-value and chiral carbohydrate from a BBA

under mild conditions because of the substrate-specificity, enantiocontrol and cascade transformation enabled by enzymes.[32] However, very few enzymes are able to "handle" formaldehyde due to its high reactivity toward several nucleophilic residues of enzymes leading to deactivation and eventually denaturation.[16c] The large exploration and development of D-fructose-6-phosphate aldolase (FSA) and its mutants, in the past 20 years, led to key substrate-specificity in aldol reactions.[33] This made FSA a biocatalyst of choice to perform aldol additions to formaldehyde with high efficiency and uncompromised stereochemical fidelity..[34] Concerning the formose reaction, enzymatic-catalysis is in its infancy. While no natural enzyme is known to catalyze such transformation, benzaldehyde lyase (BAL) from *Pseudomonas fluorescens* biovar I, was recently engineered to catalyze the oligomerization of formaldehyde into GA and dihydroxyacetone (DHA).[35] This variant, named formolase (FLS), contains seven mutations necessary to adjust the active site - composed of the carbenic center of the co-enzyme thiamine pyrophosphate (TPP) – for the transformation of formaldehyde instead of the natural substrate benzaldehyde. Thanks to this key carbenic active center, the enzyme promotes the asymmetric umpolung activation of a formaldehyde molecule that enables carbon-carbon ligation with a second and eventually a third formaldehyde equivalent leading to the formation of dihydroxyacetone.[16c]

With these powerful tools in hands, we thus aimed at developing a new hybrid chemo-enzymatic catalytic system for the transformation of CO_2 into carbohydrates *via* the intermediacy of formaldehyde.[36] Herein, we disclose the selective reductive oligomerization of CO_2 into C_3 (DHA) and C_4 (L-erythrulose) carbohydrates (Scheme 1d). These sequential reactions are unprecedented and proceed with perfect stereocontrol for the latter carbohydrate. The key aspect of the work was to ensure the compatibility and complementarity between the product of the chemical CO_2 reduction step and the enzymatic C-C coupling step.[37]

RESULTS AND DISCUSSION

Selective 4e$^-$ reduction of CO_2 by hydroborane. As indicated in the introduction, only four BBA (**BBA-1-4**, Scheme 1c) were obtained selectively from the hydroboration of CO_2.[38] However, we believed that the instability of **BBA-1** and **BBA-2** and the structural complexity of **BBA-3** and **BBA-4** with pendant Lewis basic moieties would not be adapted for the development of a hybrid catalytic system. We thus aimed at synthesizing a new bis(boryl)acetal, compound **1**, featuring dimesitylboryl moieties. 1 atm of CO_2 was subjected to hydroboration with dimesitylborane ($HBMes_2$) in the presence of 1 mol% of $Fe(H)_2(dmpe)_2$ that we previously used for the selective generation of **BBA-1** with 9-BBN (Scheme 2).[22c] The corresponding bis(boryl)acetal, compound **1,** was generated selectively after 1 hour at room temperature in THF-d_8. The yield was measured *in situ* at 75%, while the 2e$^-$ reduction product (formoxyborane) was measured at 19% yield and the quantity of the over-reduced product (methoxyborane) remained negligible. The selectivity for the 4e$^-$ reduction product enabled by this [Fe] catalyst is noticeable as our previous study showed that only 9-BBN led to such selectivity with this catalyst in contrast to HBpin or HBCat.[22c] Compound **1** is stable in solution and in the solid state for several months under an inert atmosphere of Ar, in marked contrast with the reported compounds **BBA-1** and **BBA-2** (Scheme 1c). We thus sought for isolating it. When the orange solution of a larger scale synthesis was concentrated and placed at -21 °C overnight, compound **1** was isolated as colorless crystals in 69% yield (301 mg, 0.55 mmol). The ^{13}C-labelled analogue could also be generated and isolated in 65% yield (284 mg, 0.52 mmol). The characteristic methylene signal appeared at 5.49 and 89.6 ppm in ^{1}H and ^{13}C{^{1}H} NMR analyses in THF-d_8, respectively. The $^1J_{H\text{-}C}$ coupling constant was measured at 165.3 Hz. These chemical shifts and coupling constant appear in the specific narrow range of methylene NMR characterization for the reported BBA.[22a, 26-27, 29-30] The isolated crystals were suitable for X-Ray diffraction analysis showing the expected doubly borylated acetal moiety (Figure 1). The molecule crystallized in a centrosymmetric monoclinic C2/c system centered at the carbon atom of the methylene moiety. The structural data can be compared to **BBA-3** and **BBA-4**, the only structurally characterized BBA compounds (Scheme 1c).[29-30] While the C-O bond distances of 1.413(18) Å are at a lower range compared to the analogous distances of **BBA-3** (1.426(2) and 1.414(2) Å) and **BBA-4** (1.418(3) and 1.415(3) Å), the B-O bond distance of 1.366(2) Å is at an upper range compared to **BBA-3** (1.361(2), 1.354(2) Å) and **BBA-4** (1.354(3) and 1.359(3) Å). The X-Ray characterization of compound **1** proves that the mesityl moiety is sufficient for the electronic and steric stabilization of this kind of species and thus that a pendant Lewis base is not an absolute requirement. Moreover, the isolation of pure compound **1** and of its ^{13}C-labelled analogue **1-^{13}C** was a key aspect to optimize the enzymatic catalysis and to incorporate ^{13}C isotope in high value molecules.

Release of formaldehyde from compound 1. Having isolated compound **1**, we hoped that the observed stability would not be detrimental for its reactivity as a formaldehyde provider. In addition, the conditions of formaldehyde release should be compatible with enzymatic transformations which are usually conducted in aqueous buffer solutions. Satisfyingly, the addition of 10 equiv. of D_2O at room temperature in a THF-d_8 solution of compound **1** led to a large release of formaldehyde in the form of monomeric formaldehyde, methylenediol and related oligomers in less than 2 hours (Scheme 2, Figures S8-S10).[39] Labeling experiment using $^{13}CO_2$ confirmed that the release occurred from compound **1** (Figures S10-11). As a comparison, **BBA-1** releases formaldehyde slightly faster (30 min) in the same conditions,[20] while a related bis(silyl)acetal was reported to be hydrolyzed in DMSO at 100 °C.[31a, 40] Furthermore, ^{13}C-labelled imine (**2**, 80% yield with respect to the initial amount of **1-^{13}C** hydrolyzed) was formed when an excess of bis(diisopropyl)aniline was added to the medium (Scheme 2, Figure S16).[41] This proved the availability of the released formaldehyde equivalents ("H^{13}CHO") from **1** for further transformations.

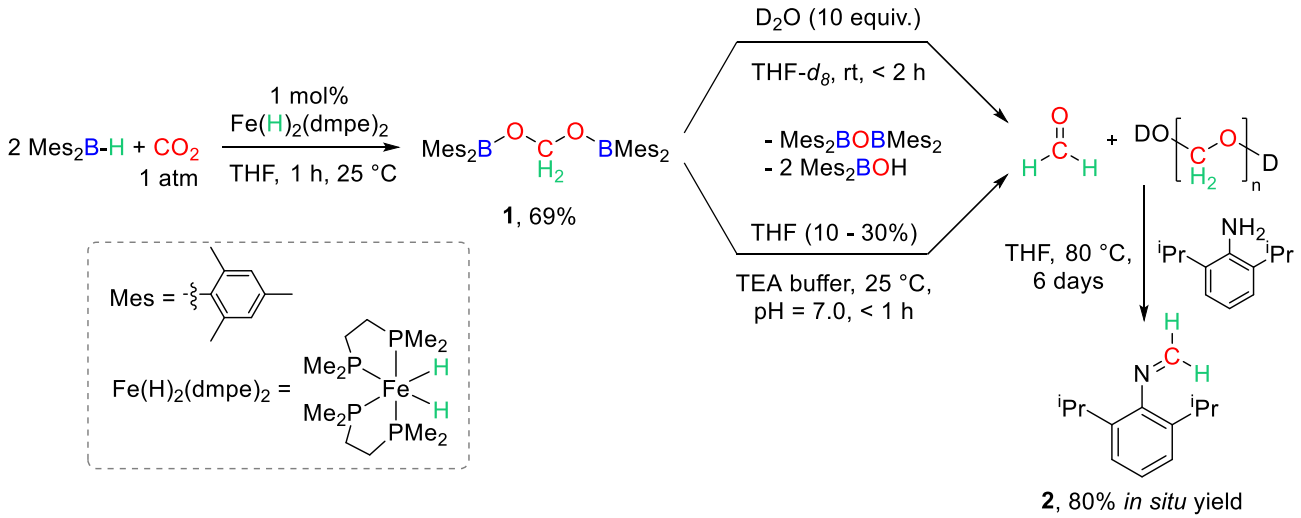

Scheme 2. Selective synthesis of compound 1 and hydrolysis pathways leading to formaldehyde release and generation of compound 2

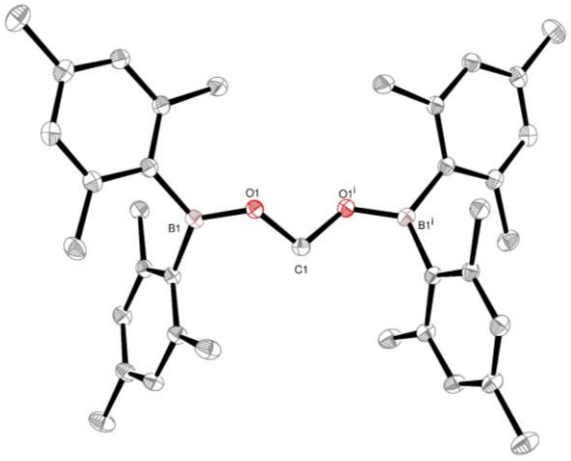

Figure 1. ORTEP view of X-ray structure of **1** at 50% thermal ellipsoid probability level. All the hydrogen atoms were omitted for clarity. Selected bond distances (Å) and angles (°): B1-O1 1.366(2), O1-C1 1.413(18), O1-C1-O_1^i 106.36(18).

This first test of hydrolysis in organic solvent was complemented by tests in aqueous solutions and notably in the buffer solution that will be used for the enzymatic transformation. In pure H_2O, compound **1** is not soluble and remains unreacted after 2 months in suspension. In an aqueous triethanolamine buffer solution (TEA, 25 mM, pH 7.0) containing $MgSO_4$ (1 mM) and TPP co-factor (0.1 mM), compound **1** released 14 and 57% of formaldehyde after 24 and 48 h, respectively. The addition of 10, 20 and 30% v/v of THF, led to a faster release of 51, 78 and 95%, respectively, after 1 h. As shown in Table S1, the amount of released formaldehyde appears to readily reach a plateau for each % of THF (< 1 h). However, care must be taken since formaldehyde was quantified by HPLC in these conditions which might not consider its possible reactivity with the buffer solution overtime in function of the amount of THF.

Enzymatic transformation of compound 1 into DHA (3) and L-erythrulose (4)

We produced the FLS enzyme and verified that it exhibits the expected activity in the oligomerization of commercial formaldehyde solution into **3** (Table S3).[35] We systematically repeated this control reaction in parallel of every enzymatic-catalysis described hereafter to ensure about the activity of the enzyme. In addition, we also verified that no formation of **3** occurred in absence of the enzyme. FLS could be stored at 4 °C and without significant loss of activity over 7 days (Figure S17). Since THF appears to promote the release of formaldehyde from compound **1**, the stability of FLS in the presence of organic co-solvents (5-30%) was evaluated by differential scanning fluorimetry (DSF), which measures the thermal unfolding of proteins and calculate the enzyme melting temperature (T_m) in the assayed conditions (Figure S18).[42] The T_m (55.7 °C) of FLS (obtained in TEA buffer (25 mM, pH 7.0 with 1 mM $MgSO_4$ and 0.1 mM TPP) decreases with increasing concentration of DMF, acetonitrile and methanol which is indicative of loss of the supramolecular structure of the enzyme. Interestingly, FLS structure proved to be stable in THF and DMSO according to this analysis. In the presence of up to 30% of THF – the solvent of interest for the enzymatic transformation – the variation of the T_m value is lower than 0.4 °C.[43] The FLS-catalyzed formose reaction was then tested with commercial formaldehyde solution in the presence of 10 and 20% THF. While formaldehyde was efficiently transformed into **3** within 24 h with a 99% yield in the presence of 10% THF, only 11% yield was measured in the presence of 20% THF (Table S3). Since the DSF experiment proved that up to 30% THF does not unfold FLS, we assume that THF might modify the ionization state of the enzyme or its active site, affecting its activity or operational stability at long incubation times.

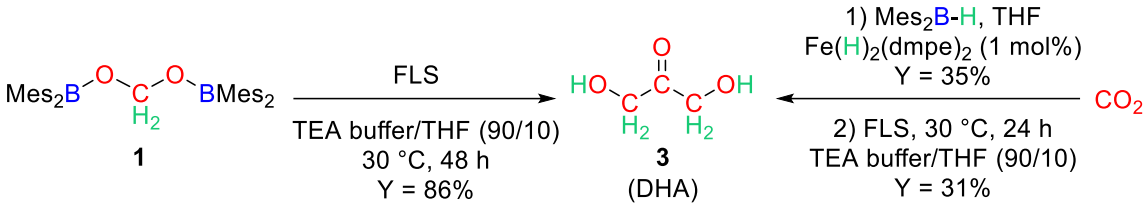

Scheme 3. Generation of 3 from FLS-catalyzed formose reaction of 1 isolated or generated *in situ* from CO_2

Table 1. FLS-catalyzed trimerization of 1 into 3

Entry	Conditions[a]	Yield (%) of **3**						
		< 1 min	1 h	2 h	4 h	7 h	24 h	48 h
1	0% THF	0	0	0	0	0	3 ± 2	4 ± 2
2	10% THF	0	3 ± 2	9 ± 7	20 ± 7	40 ± 3	77 ± 2	86 ± 4
3	20% THF	2 ± 2	7 ± 1	15 ± 2	21 ± 3	32 ± 2	38 ± 4	55 ± 1
4	30% THF	0	0	0	0	0	0	0
5	15% THF/5% MeOH	0	40 ± 1	48	64 ± 2	72 ± 2	76	66 ± 2
6[b]	0% THF	0	0	0	0	0	2 ± 1	3
7[b]	10% THF	0	1	2	6 ± 1	10 ± 1	42 ± 1	72 ± 1

[a]Reaction mixture (0.8 mL) containing FLS (20 μM), **1** (10 mM, unless otherwise stated) and TEA buffer (25 mM, pH 7.0) with 1 mM $MgSO_4$ and 0.1 mM TPP. [b]Similar conditions but with 25 mM of **1.** Each experiment was performed in triplicate except for Entry 6, which was obtained in duplicate.

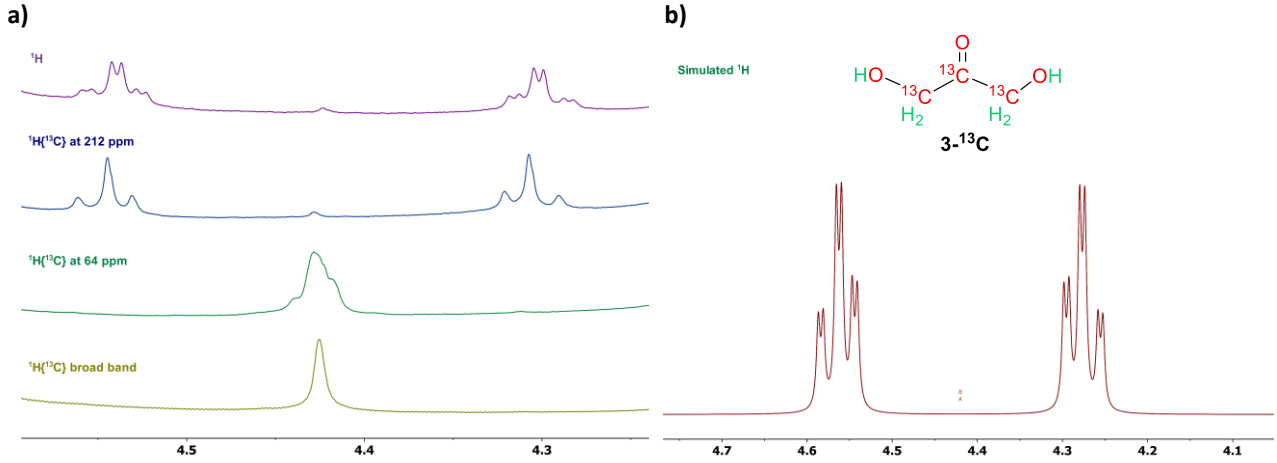

Figure 2. ^1H NMR characterization of the methylene moiety of **3-^{13}C**: a) stack from bottom to top: ^1H with broad band ^{13}C decoupling, selective ^{13}C-decoupling at 65 ppm, selective ^{13}C-decoupling at 212 ppm and ^1H without any decoupling, b) simulated ^1H NMR spectrum.

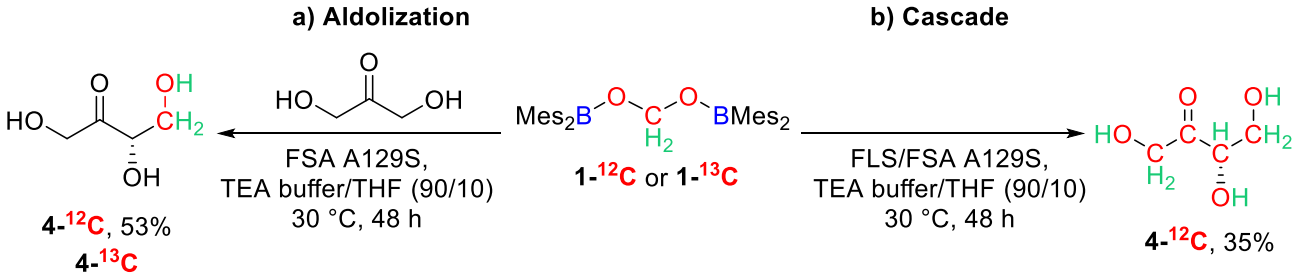

Scheme 4. Synthesis of L-erythrulose (4 or 4-^{13}C) from: a) FSA-catalyzed aldolization reaction between 1 or 1-^{13}C and commercial DHA, b) FLS/FSA A129S catalytic one-pot cascade transformation of compound 1

The FLS-catalyzed oligomerization of compound **1** into **3** was then probed in different solvent conditions (Scheme 3 and Table 1). Satisfyingly, formaldehyde released from compound **1** was converted into **3** in a very selective manner with an *in situ* yield up to 86% in the best conditions: TEA buffer solution/THF (90/10) after 48 h at 30 °C (Table 1, Entry 2). Lower *in situ* yields of 55% and 0% were obtained using 20 and 30% THF, respectively after 48 h (Table 1, Entries 3 and 4 respectively). Hence, 10% v/v of THF appeared to offer a good balance between the solubilization of **1** for an efficient formaldehyde release and limiting the impact of organic co-solvent on the activity of the enzyme as we have shown that 20 and 30% THF are detrimental to FLS activity with commercial formaldehyde (see Table S3). Negligible amount of product was detected when using pure aqueous buffer media (Table 1, Entry 1). We also probed a mixture of 15% THF/5% MeOH to test if a small amount of methanol, known to stabilize formaldehyde in an acetal form, would strongly impact the reaction. A 66% yield was observed in these conditions showing a slight increase compared to 20% THF but lower than when using 10% THF (Table 1, Entries 5 *versus* 3 and 2, respectively). Higher concentration of **1** (*i.e.* 25 mM instead of 10 mM) afforded lower yields (72% with 10% THF), whereas a negligible amount of product was detected in the absence of THF (Table 1, Entries 6 and 7, respectively).

We conducted the same reaction starting from ^{13}C-labelled **1** and observed the *in situ* formation of fully ^{13}C-labelled DHA (**3-^{13}C**), characterized in ^{13}C{^{1}H} NMR by two signals at δ 212.1 (t, $^{1}J_{C\text{-}C}$ = 41.6 Hz) and 64.1 (d, $^{1}J_{C\text{-}C}$ = 41.4 Hz) for the carbonyl and methylene fragments, respectively. The ^{1}H NMR spectrum exhibited a second order coupling signal for the methylene moiety due to a significant $^{2}J_{C\text{-}C}$ coupling between the two methylene-carbon nuclei (top spectrum, Figure 2a). This signal could be simulated as an AA'BB'CC'D system with a $^{2}J_{C\text{-}C}$ = 20 Hz in addition to the observed $^{1}J_{C\text{-}H}$ = 143.0 Hz, $^{2}J_{C\text{-}H}$ = 3.0 Hz and $^{1}J_{C\text{-}C}$ = 41.4 Hz (Figure 2b). The connectivity between the different nuclei was further evidenced by selective ^{13}C-decoupling at δ 212 and 64 (Figure 2a, middle spectra), while broad band ^{13}C-decoupling resulted in an expected singlet signal (Figure 2a, bottom spectrum). More importantly, limited amount of ^{12}C-labelled DHA (<5%) could be observed in ^{1}H NMR analysis of the crude mixture proving that the DHA yield measured by HPLC arises from the bis(boryl)acetal compound **1** and thus from CO_2.

The chemo-enzymatic one-pot reaction from CO_2 also led to the synthesis of **3**, albeit with a modest 31% yield after 24 h (Table S4). This can be explained by the less efficient hydroboration step which led only to a 35% yield in compound **1**. In order to adjust the concentration of **1** in the enzymatic transformation, the hydroboration step was indeed conducted with a concentration of 0.27 M of $HBMes_2$ instead of 0.08 M in the optimized standard reaction. We believe that the remaining $HBMes_2$ is detrimental for FLS activity or can react with the product of the reaction. Moreover, unexplained early conversion was observed within 1 min with a measured yield of 23% in **3** (Table S4).[44]

Aiming at increasing the chain length of the generated carbohydrate and more importantly at generating a chiral center with perfect enantiocontrol, we turned our attention to enzymatic cascade reaction. The mono-mutant A129S of FSA was shown to catalyze the aldol reaction between DHA and formaldehyde with perfect enantiocontrol.[33] We produced this mutant and used it first to catalyze the aldol reaction between **1** and commercial DHA. Interestingly, the expected L-erythrulose **4** was generated with an *in situ* yield of 53% after 48 h (Scheme 4a, Table S7), which is slightly lower than the estimated 80% conversion from the reaction between commercial formaldehyde and DHA.[45] This reaction proved that compound **1** can also be used as a formaldehyde surrogate in enzymatic aldol reactions. Moreover, L-erythrulose **4-^{13}C**, featuring a $^{13}CH_2$ moiety was prepared by reacting **1-^{13}C** with commercial DHA (Scheme 4a). Semi-preparative HPLC enabled to isolate **4-^{13}C** in 17% yield. Although the unoptimized isolation method and the small scale used (2.4 mg, 20 μmol) explain this modest yield (*in situ* yield was measured at 57%, in accordance with the synthesis of **4**), the main goal pursued in isolating **4-^{13}C** was to confirm the perfect enantioselectivity of the reaction. Satisfyingly, the measured optical rotation of the molecule ($[\alpha]_D^{25}$: + 11 (*c* 0.00105, H_2O)) is comparable with the reported value[45b] ($[\alpha]_D^{25}$: + 12 (c 1.0, H_2O)) and is a perfect match with the measurement of a commercial sample of **4** under identical conditions ($[\alpha]_D^{25}$: + 11 (*c* 0.001, H_2O)).

Having proven that **1** could be involved i) in the FLS-catalyzed formose reaction to produce DHA and ii) in the enantioselective FSA A129S-catalyzed aldol reaction with commercial DHA to produce L-erythrulose, we then combined both reactions in an enzymatic cascade. Such FLS/FSA A129S cascade was recently developed with commercial formaldehyde.[46] To our delight the FLS/FSA A129S-catalyzed cascade reaction could be conducted with **1** as the unique source of carbon to generate L-erythrulose with an equimolar ratio of 20 μM of both enzymes. Compound **4** was generated in 35% yield (Scheme 4b, Table S8) when **1** and both enzymes were placed in the buffer solution containing 10% THF at the beginning of the reaction. As in the case of the reported cascade,[46] L-glyceraldehyde and DHA were observed in 15 and 13% yields, respectively, while compound **4** featuring four carbon atoms arising from **1** and thus from CO_2 remains the major product of the reaction.

CONCLUSION

In the present study, we performed the first cell-free enantioselective transformation of the carbon atom of CO_2. This is a fundamental achievement as it relates to the natural transformation of CO_2. Moreover, DHA and L-erythrulose are of interesting value as products or precursor for the cosmetic (as tanning agent), fine chemical, pharmaceutical, and food industries.[47] On the application point of view, the access to carbohydrates from CO_2 enables to incorporate different carbon isotope as was proven herein with the synthesis of **3-^{13}C** and **4-^{13}C**.

While we previously explored similar formaldehyde two-step strategy by chemical means-only, this challenging, yet powerful route, is largely enhanced by the use of an original hybrid chemo-enzymatic catalytic system. As such, we believe that the present transformation of CO_2 into C_3 and chiral C_4 carbohydrates is unprecedented in terms of complexity gain. The specificity and enantiocontrol offered by FLS and FSA A129S indeed enabled the control of the chain length and of the chirality of the synthesized compounds. The key aspect to develop such a hybrid system was to ensure the compatibility between i) the Fe-catalyzed hydroboration of CO_2 with the synthesis of an isolable yet readily hydrolyzable bis(boryl)acetal compound **1** and ii) an enzymatic transformation able to tolerate organic co-solvent.

On a broader perspective, although the reduction step with the hydroborane is not atom-economical, this is to be related to the large energy input and atom expense (ATP and NADPH) required by bio-organisms for the reduction of CO_2.[48] Our results show that an organometallic reduction step can be coupled with an enzymatic step in such transformation. There is large

room for improvements of the yield, selectivity and compatibility that should fuel further developments of each step either individually or in a combined way in order to expand the scope of accessible carbohydrates from CO_2.

EXPERIMENTAL SECTION

General information

Manipulations were performed using a combination of glovebox, high vacuum and Schlenk techniques under an argon atmosphere for the synthesis of compound 1 (BBA^{Mes}) and in open vessel for the biocatalytic transformations. When required solvents were dried through an activated alumina purification system (MBraun SPS-800) and degassed by standard procedure. Quick Pressure Valve NMR tubes and Fisher-Porter tubes were used for the reactions with CO_2. NMR spectra were recorded on Bruker machines: QV500, AV400 or AV300 spectrometers. Deuterated solvents were freeze-pump-thaw degassed and stored over 4 Å molecular sieves under argon. All chemical shifts for ^1H and ^{13}C are relative to $SiMe_4$. Chemical shifts are given in ppm and coupling constants in Hz. The following abbreviations are used: s, singlet; d, doublet; dd, doublet of doublets; t, triplet; m, multiplet. Infrared spectra were recorded on a Perkin Elmer 1725 Spectrometer. Elemental analyses were performed by the "in-house" service of the Laboratoire de Chimie de Coordination, Toulouse, on a Perkin Elmer 2400 Series II Analyze fitted with a catharometer. Specific rotations were measured with a Perkin-Elmer 241 Polarimeter. $Fe(H)_2(dmpe)_2$[49] and Mes_2BH[50] were prepared according to literature procedures. Thiamine pyrophosphate chloride (TPP), formaldehyde (37 wt %), GA, DHA, L-erythrulose and L-glyceraldehyde were purchased from Merck and used as received. Synthetic oligonucleotides were purchased from Eurogentec. Milli-Q grade water was used for analytical and semi-preparative HPLC. Bacterial strains, oligonucleotides and plasmids used in this study are listed in Table S2.

Analytical HPLC was performed on a Bio Rad Aminex HPX-87H, 300 x 7.8 mm column. Samples (20 µL) were injected and eluted with the following conditions: isocratic solvent system 5 mM aqueous sulfuric acid (H_2SO_4) solution, 30 minutes run time per sample, flow rate 0.5 mL.min^{-1}, detection using both Refractive Index (RI) and Ultraviolet (UV) at 192 nm detectors, column temperature 26 °C. The amount of product was quantified from the peak areas and calibration curves (see ESI section 1.3 for details). Formaldehyde was detected by the RI detector while the other compounds analyzed were detected by UV.

Synthesis of compound 1

A Fisher-Porter bottle was charged with Mes_2BH (400 mg, 1.6 mmol), $Fe(H)_2(dmpe)_2$ (5.7 mg, 0.016 mmol) and 4 mL of anhydrous THF. The argon atmosphere was replaced by 1 atmosphere of CO_2. After 3 min, the Fisher-Porter was closed and the mixture was stirred at 25 °C for 1 hour. The resulting orange solution was cannula filtered into a Schlenk flask and concentrated under reduced pressure to half of the initial volume. The Schlenk flask was then placed at – 21 °C for 12 hours during which time, colorless shinny crystals precipitated. After removing the supernatant and washed the crystals with cold Et_2O (4 x 1 mL) at -20 °C, crystals were dried under reduced pressure affording compound **1** as a white solid in 69% yield (301 mg, 0.55 mmol). The ^{13}C-isotopologue of **1** was obtained using $^{13}CO_2$ following the procedure described above. The product was obtained as a fluffy white solid in 65% yield (284 mg, 0.52 mmol).

***In situ* generation of 1**

An NMR tube was charged with Mes_2BH, $Fe(H)_2(dmpe)_2$ (1 mol%), hexamethylbenzene as internal standard (10 mol%) and THF-d_8 (*ca.* 0.6 mL). The solution was degassed and placed under 1 atmosphere of CO_2 (or $^{13}CO_2$) for 3 minutes. The mixture turned instantaneously orange upon introduction of CO_2. The tube was then closed and placed at 25 °C for 50 minutes affording a clear orange solution. A 75% yield of **1** was determined by ^1H NMR spectroscopy against internal standard.

^1H NMR (THF-d_8, 298 K, 400 MHz): δ 6.72 (s, 8H, CH_{ar}), 5.49 (s, 2H, OCH_2O), 2.21 (s, 12H, p-CH_3), 2.15 (s, 24H, o-CH_3); **$^{11}B\{^1H\}$ NMR** (THF-d_8, 298 K, 128 MHz): δ 48.5; **$^{13}C\{^1H\}$ NMR** (THF-d_8, 298 K, 101 MHz): δ 141.8 (*C*-ortho), 139.5 (*C*-para), 136.0 (*C*-ipso), 129.1 (*C*-meta), 89.6 (*C*H_2), 22.8 (o-*C*H_3), 21.3 (p-*C*H_3). Elemental Analysis Calculated for $C_{37}H_{46}B_2O_2$: C, 80.33; H, 9.44. Found: C, 80.35; H, 9.16. Melting temperature: 155 °C.

1-^{13}C: **^1H NMR** (THF-d_8, 298 K, 400.0 MHz): δ 5.48 (d, 2H, $^1J_{CH}$ = 165.3 Hz, OCH_2O); **$^{13}C\{^1H\}$ NMR** (THF-d_8, 298 K, 101 MHz): δ 89.6 (O*C*H_2O).

Synthesis of Mes_2BOH

A J. Young NMR tube was charged with Mes_2BH (10 mg, 0.04 mmol) and 0.6 mL of THF-d_8. Degassed H_2O (1.5 µL, 0.08 mmol) was added to the THF solution at room temperature. Immediate bubbling was observed. The reaction was monitored by NMR spectroscopy which showed the quantitative conversion to Mes_2BOH after few minutes at room temperature (10.3 mg, 0.038 mmol, *in situ* yield >99%). Colorless crystals of Mes_2BOH suitable for X-Ray diffraction were obtained from slow evaporation of a saturated solution of THF.

^1H NMR (THF-d_8, 298 K, 400 MHz): δ 9.09 (s, 1H, BO*H*), 6.71 (s, 4H, CH_{ar}), 2.20 (s, 18H, CH_3); **$^{11}B\{^1H\}$ NMR** (THF-d_8, 298 K, 128 MHz): δ 47.8; **$^{13}C\{^1H\}$ NMR** (THF-d_8, 298 K, 101 MHz): δ 141.6 (o-*C*), 138.5 (p-*C*), 128.8 (m-*C*H), 137.6 (ipso-*C*), 22.8 (o-*C*H_3), 21.3 (p-*C*H_3).

This compound was synthesized and crystallized with different cell parameters earlier. [51]

Synthesis of 3 from FLS-catalyzed formose reaction of 1

The reactions were performed in a reaction mixture (0.8 mL) containing FLS (20 µM), compound **1** (10 mM, unless otherwise stated) and TEA buffer (25 mM, pH 7.0) containing 1 mM $MgSO_4$ and 0.1 mM TPP. 10, 20 and 30% THF were added when required. The order of addition of the reaction components were the following: i) **1**, ii) THF, iii) TEA buffer and iv) FLS. The samples were placed at 30 °C and shaken at 900 rpm. Aliquots of 0.1 mL were taken after 0, 1, 2, 4, 7, 24 and 48 hours. The aliquots were heated at 98 °C for 3 minutes, centrifuged for 2 minutes at 12 000 x g and the supernatant solution was analyzed by analytical HPLC. Each experiment was performed as triplicate unless otherwise stated. The results obtained are reported in Table 1.

Synthesis of 4-^{13}C from FSA A129S-catalyzed aldol condensation between commercial DHA and 1-^{13}C

1-^{13}C (65 mg, 0.12 mmol, 10 mM for a final volume of 12 mL) was dissolved in 1.2 mL of THF (10% THF). DHA (11 mg, 0.12 mmol, 10 mM) was added followed by TEA buffer (25 mM, pH 7.0) containing 1 mM $MgSO_4$ and 0.1 mM TPP. Then FSA A129S (20 µM) was added to the mixture. The reaction mixture was shaken at 190 rpm and 30 °C. The reaction was monitored by analytical HPLC (aliquots were taken overtime, heated at 98 °C for 3 minutes, centrifuged for 2 minutes at 12 000 x g and the supernatant solution analyzed by HPLC). A white solid precipitated from the reaction mixture during the reaction. After 5 days, no more increase in L-erythrulose yield (57% yield) was measured by HPLC (unreacted DHA remained in the reaction mixture). MeOH (12 mL) was added and the mixture was centrifuged (11 000 rpm, 10 °C, 30 min). After filtration and removal of the volatiles (THF and MeOH) under a stream of air the resulting solution was lyophilized. The crude material (300 mg, pale yellowish oil) was purified by semi-preparative HPLC.

The fractions containing the compound of interest were combined, the volatiles removed under a stream of air and the resulting solution lyophilized. L-erythrulose (**4-^{13}C**) was obtained as a pale-yellow oil in an isolated yield of 17% (2.4 mg, 20 µmol). A white precipitate was recovered, dried under reduced pressure and analyzed by NMR spectroscopy (42 mg recovered as a white solid). The white solid was identified as the borylated by-product Mes_2BOH.

^{1}H NMR (D_2O, 298 K, 400 MHz): δ 4.55 (m, 2H, CH_2), 4.46 (m, 1H, CH), 3.87 (m, 2H, ^{13}CH_2). **^{13}C{^{1}H} NMR** (D_2O, 298 K, 101 MHz): δ 62.8 (s, ^{13}C-**4**). $[\alpha]_D^{25}$: + 11 (*c* 0.00105, H_2O) [commercial L-erythrulose sample recorded in the same conditions: $[\alpha]_D^{25}$: + 11 (*c* 0.001, H_2O)].

Synthesis of 4 from 1 via the FLS/FSA A129S cascade reaction

The cascade reaction was performed in a reaction mixture (0.8 mL) containing FLS and FSA A129S (20 µM each), 10 mM of **1** and TEA buffer (25 mM, pH 7.0) containing 1 mM $MgSO_4$ and 0.1 mM TPP with 10% THF. The order of addition of the reaction components were the following: i) **1**, ii) THF, iii) TEA buffer, iv) FSA A129S and v) FLS. The samples were placed at 30 °C and 900 rpm. Aliquots of 0.1 mL were taken after 0, 1, 2, 4, 7, 24 and 48 hours (see Table S8). The aliquots were heated at 98 °C for 3 minutes, centrifuged for 2 minutes at 12 000 x g and the supernatant solution was analyzed by analytical HPLC.

ASSOCIATED CONTENT

SUPPORTING INFORMATION

NMR and IR spectra, representative HPLC chromatograms, Table of results (S1-S9) as well as further experimental details can be found in supporting information. CCDC numbers for compound **1** and Mes_2BOH was deposited on the CCDC data base under these numbers: 2097924 and 2097925, respectively. "This material is available free of charge via the Internet at http://pubs.acs.org."

AUTHOR INFORMATION

Corresponding Author

*Email: sarah.desmons@gmail.com, sebastien.bontemps@lcc-toulouse.fr

Author Contributions

The manuscript was written through contributions of all authors. All authors have given approval to the final version of the manuscript.

ACKNOWLEDGMENT

We wish to thank the reviewers, who's comments helped to improve the manuscript and in particular the ^{1}H NMR interpretation of compound **3-^{13}C**. S. D. thanks Région Midi-Pyrénées and Université Fédérale de Toulouse for doctoral fellowship. S. B. thanks the ANR programme JCJC "ICC". C. Bijani is gratefully acknowledge for his help on the simulation of **3-^{13}C**. K.G.-S., C. D. and R. F. thank the Carnot 3BCAR (project SUCRES), including the fellowship of K. G.-S. R. F. thanks the Mission for Transversal and Interdisciplinary Initiatives of the CNRS (project CASCADE). We gratefully thank N. Monties, S. Pizzut and M. Guicherd for technical assistance in HPLC experiments, G. Cioci for assistance in DSF experiments and protein purification and the ICEO facility dedicated to enzyme screening and discovery, part of the Integrated Screening Platform of Toulouse (PICT, IBiSA). DSF is part of the Integrated Screening Platform of Toulouse (PICT, IBiSA. We thank S. Heux and A. De Simone for the generous gift of plasmid containing the gene encoding for FLS. Finally, J. Durand is gratefully acknowledged for his help on isolating compound **4-^{13}C** by semi-preparative HPLC.

REFERENCES

1. (a) Stallforth, P.; Lepenies, B.; Adibekian, A.; Seeberger, P. H. Carbohydrates: A Frontier in Medicinal Chemistry. *J. Med. Chem.* **2009,** *52*, 5561-5577; (b) Weymouth-Wilson, A. C. The role of carbohydrates in biologically active natural products. *Nat. Prod. Rep.* **1997,** *14*, 99-110.

2. (a) de Meirelles, J. L.; Nepomuceno, F. C.; Peña-García, J.; Schmidt, R. R.; Pérez-Sánchez, H.; Verli, H. Current Status of Carbohydrates Information in the Protein Data Bank. *J. Chem. Inf. Model.* **2020,** *60*, 684-699; (b) DeMarco, M. L.; Woods, R. J. Structural glycobiology: a game of snakes and ladders. *Glycobiology* **2008,** *18*, 426-440; (c) Bertozzi, C. R.; Kiessling; L., L. Chemical Glycobiology. *Science* **2001,** *291*, 2357-2364.

3. (a) Mlynarski, J.; Gut, B. Organocatalytic Synthesis of Carbohydrates. *Chem. Soc. Rev.* **2012,** *41*, 587-596; (b) Nicolaou, K. C.; Vourloumis, D.; Winssinger, N.; Baran, P. S. The Art and Science of Total Synthesis at the Dawn of the Twenty-First Century. *Angew. Chem. Int. Ed.* **2000,** *39*, 44-122; (c) Zhang, W.; Zhang, T.; Jiang, B.; Mu, W. Enzymatic approaches to rare sugar production. *Biotechnology Advances* **2017,** *35*, 267-274.

4. (a) Wan, Y.; Lee, J.-M. Toward Value-Added Dicarboxylic Acids from Biomass Derivatives via Thermocatalytic Conversion. *ACS Catal.* **2021,** *11*, 2524-2560; (b) Zhang, Z.; Huber, G. W. Catalytic oxidation of carbohydrates into organic acids and furan chemicals. *Chem. Soc. Rev.* **2018,** *47*, 1351-1390.

5. Northrup, A. B.; MacMillan, D. W. C. Two-Step Synthesis of Carbohydrates by Selective Aldol Reactions. *Science* **2004,** *305*, 1752-1755.

6. (a) Frihed, T. G.; Bols, M.; Pedersen, C. M. Synthesis of l-Hexoses. *Chem. Rev.* **2015,** *115*, 3615-3676; (b) Li, Z.; Gao, Y.; Nakanishi, H.; Gao, X.; Cai, L. Biosynthesis of rare hexoses using microorganisms and related enzymes. *Beilstein J. Org. Chem.* **2013,** *9*, 2434-2445; (c) Beerens, K.; Desmet, T.; Soetaert, W. Enzymes for the biocatalytic production of rare sugars. *Journal of Industrial Microbiology and Biotechnology* **2012,** *39*, 823-834.

7. (a) Geider, R. J.; Delucia, E. H.; Falkowski, P. G.; Finzi, A. C.; Grime, J. P.; Grace, J.; Kana, T. M.; Roche, J. L.; Long, S. P.; Osborne, B. A.; Platt, T.; Prentice, I. C.; Raven, J. A.; Schlesinger, W. H.; Smetacek, V.; Stuart, V.; Sathyendranath, S.; Thomas, R. B.; Vogelmann, T. C.; Williams, P.; Woodward, F. I. Primary productivity of planet earth: biological determinants and physical constraints in terrestrial and aquatic habitats. *Global Change Biology* **2001,** *7*, 849-882; (b) Beer, C.; Reichstein, M.; Tomelleri, E.; Ciais, P.; Jung, M.; Carvalhais, N.; Rödenbeck, C.; Arain, M. A.; Baldocchi, D.; Bonan, G. B.; Bondeau, A.; Cescatti, A.; Lasslop, G.; Lindroth, A.; Lomas, M.; Luyssaert, S.; Margolis, H.; Oleson, K. W.; Roupsard, O.; Veenendaal, E.; Viovy, N.; Williams, C.; Woodward, F. I.; Papale, D. Terrestrial Gross Carbon Dioxide Uptake: Global Distribution and Covariation with Climate. *Science* **2010,** *329*, 834-838; (c) Buick, R. When did oxygenic photosynthesis evolve? *Phil. Trans. R. Soc. B* **2008,** *363*, 2731-2743.

8. (a) Singh, J.; Pandey, P.; James, D.; Chandrasekhar, K.; Achary, V. M. M.; Kaul, T.; Tripathy, B. C.; Reddy, M. K. Enhancing C_3 photosynthesis: an outlook on feasible interventions for crop improvement. *Plant Biotech. J.* **2014,** *12*, 1217-1230; (b) Erb, T. J.; Zarzycki, J. A short history of RubisCO: the rise and fall (?) of Nature's predominant CO_2 fixing enzyme. *Curr. Opin. Biotechnol.* **2018,** *49*, 100-107.

9. (a) Schada von Borzyskowski, L.; Carrillo, M.; Leupold, S.; Glatter, T.; Kiefer, P.; Weishaupt, R.; Heinemann, M.; Erb, T. J. An engineered Calvin-Benson-Bassham cycle for carbon dioxide fixation in Methylobacterium extorquens AM1. *Metab. Eng.* **2018,** *47*, 423-433; (b) Sundaram, S.; Diehl, C.; Cortina, N. S.; Bamberger, J.; Paczia, N.; Erb, T. J. A Modular In Vitro Platform for the Production of Terpenes and Polyketides from CO_2. *Angew. Chem. Int. Ed.* **2021,** *60*, 16420-16425; (c) Antonovsky, N.; Gleizer, S.; Noor, E.; Zohar, Y.; Herz, E.; Barenholz, U.; Zelcbuch, L.; Amram, S.; Wides, A.; Tepper, N.; Davidi, D.; Bar-On, Y.; Bareia, T.; Wernick, David G.; Shani, I.; Malitsky, S.; Jona, G.; Bar-Even, A.; Milo, R. Sugar Synthesis from CO_2 in *Escherichia coli*. *Cell* **2016,** *166*, 115-125.

10. (a) Appel, A. M.; Bercaw, J. E.; Bocarsly, A. B.; Dobbek, H.; DuBois, D. L.; Dupuis, M.; Ferry, J. G.; Fujita, E.; Hille, R.; Kenis, P. J. A.; Kerfeld, C. A.; Morris, R. H.; Peden, C. H. F.; Portis, A. R.; Ragsdale, S. W.; Rauchfuss, T. B.; Reek, J. N. H.; Seefeldt, L. C.; Thauer, R. K.;

Waldrop, G. L. Frontiers, Opportunities, and Challenges in Biochemical and Chemical Catalysis of CO_2 Fixation. *Chem. Rev.* **2013,** *113*, 6621-6658; (b) Calvin, M. Nobel Lecture: The Path of Carbon in Photosynthesis. http://www.nobelprize.org/nobel_prizes/chemistry/laureates/1961/calvin-lecture.html (accessed Thu. 26 Aug 2021); (c) Benson, A.; Calvin, M. The Dark Reductions of Photosynthesis. *Science* **1947,** *105*, 648-649; (d) Bassham, J. A.; Benson, A. A.; Calvin, M. The path of carbon in photosynthesis: VIII. The role of malic acid. *J. Biol. Chem.* **1950,** *185*, 781-787; (e) Calvin, M.; Benson, A. A. The Path of Carbon in Photosynthesis IV: The Identity and Sequence of the Intermediates in Sucrose Synthesis. *Science* **1949,** *109*, 140-142; (f) Calvin, M.; Benson, A. A. The Path of Carbon in Photosynthesis. *Science* **1948,** *107*, 476-480.

11. (a) Boutin, E.; Merakeb, L.; Ma, B.; Boudy, B.; Wang, M.; Bonin, J.; Anxolabéhère-Mallart, E.; Robert, M. Molecular catalysis of CO_2 reduction: recent advances and perspectives in electrochemical and light-driven processes with selected Fe, Ni and Co aza macrocyclic and polypyridine complexes. *Chem. Soc. Rev.* **2020,** *49*, 5772-5809; (b) Artz, J.; Müller, T. E.; Thenert, K.; Kleinekorte, J.; Meys, R.; Sternberg, A.; Bardow, A.; Leitner, W. Sustainable Conversion of Carbon Dioxide: An Integrated Review of Catalysis and Life Cycle Assessment. *Chem. Rev.* **2018,** *118*, 434-504; (c) Klankermayer, J.; Wesselbaum, S.; Beydoun, K.; Leitner, W. Selective Catalytic Synthesis Using the Combination of Carbon Dioxide and Hydrogen: Catalytic Chess at the Interface of Energy and Chemistry. *Angew. Chem. Int. Ed.* **2016,** *55*, 7296-7343; (d) Goeppert, A.; Czaun, M.; Jones, J.-P.; Surya Prakash, G. K.; Olah, G. A. Recycling of carbon dioxide to methanol and derived products - closing the loop. *Chem. Soc. Rev.* **2014,** *43*, 7995-8048; (e) Aresta, M.; Dibenedetto, A. Utilisation of CO_2 as a chemical feedstock: opportunities and challenges. *Dalton Trans.* **2007**, 2975-2992.

12. A NASA challenge was recently launched on this specific topic, see: https://www.co2conversionchallenge.org/#home (accessed Thu. 26 Aug 2021).

13. Prieto, G. Carbon Dioxide Hydrogenation into Higher Hydrocarbons and Oxygenates: Thermodynamic and Kinetic Bounds and Progress with Heterogeneous and Homogeneous Catalysis. *ChemSusChem* **2017,** *10*, 1056–1070

14. (a) Guo Xiao, W. Y., Chen Jie, Li Gongqiang, Xia Ji-Bao Recent Advances of CO_2 Fixation via Asymmetric Catalysis for the Direct Synthesis of Optically Active Small Molecules. *Chinese Journal of Organic Chemistry* **2020,** *40*, 2208-2220; (b) Vaitla, J.; Guttormsen, Y.; Mannisto, J. K.; Nova, A.; Repo, T.; Bayer, A.; Hopmann, K. H. Enantioselective Incorporation of CO_2: Status and Potential. *ACS Catal.* **2017,** *7*, 7231-7244.

15. (a) Liu, C.; Huang, W.; Zhang, J.; Rao, Z.; Gu, Y.; Jérôme, F. Formaldehyde in multicomponent reactions. *Green Chem.* **2021,** *23*, 1447-1465; (b) Meninno, S.; Lattanzi, A. Asymmetric Aldol Reaction with Formaldehyde: a Challenging Process. *Chem. Rec.* **2016,** *16*, 2016-2030; (c) Reuss, G.; Disteldorf, W.; Gamer, A. O.; Hilt, A., *Formaldehyde in Ullmann's Encyclopedia of Industrial Chemistry, Wiley, Weinheim*. 2003.

16. (a) Butlerow, A. Formation synthétique d'une substance sucrée. *C. R. Acad. Sci., Paris* **1861,** *53*, 145-147; (b) Delidovich, I. V.; Simonov, A. N.; Taran, O. P.; Parmon, V. N. Catalytic Formation of Monosaccharides: From the Formose Reaction towards Selective Synthesis. *ChemSusChem* **2014,** *7*, 1833-1846; (c) Desmons, S.; Fauré, R.; Bontemps, S. Formaldehyde as a Promising C_1 Source: The Instrumental Role of Biocatalysis for Stereocontrolled Reactions. *ACS Catal.* **2019,** *9*, 9575-9588.

17. (a) Ruiz-Mirazo, K.; Briones, C.; de la Escosura, A. Prebiotic Systems Chemistry: New Perspectives for the Origins of Life. *Chem. Rev.* **2014,** *114*, 285-366; (b) Noe, C. R.; Freissmuth, J.; Richter, P.; Miculka, C.; Lachmann, B.; Eppacher, S. Formaldehyde-A Key Monad of the Biomolecular System. *Life* **2013,** *3*, 486-501.

18. Baly, E. C. C.; Heilbron, I. M.; Barker, W. F. CX.—Photocatalysis. Part I. The synthesis of formaldehyde and carbohydrates from carbon dioxide and water. *J. Chem. Soc., Trans.* **1921,** *119*, 1025-1035.

19. (a) Calvinho, K. U. D.; Laursen, A. B.; Yap, K. M. K.; Goetjen, T. A.; Hwang, S.; Murali, N.; Mejia-Sosa, B.; Lubarski, A.; Teeluck, K. M.; Hall, E. S.; Garfunkel, E.; Greenblatt, M.; Dismukes, G. C. Selective CO_2 reduction to C_3 and C_4 oxyhydrocarbons on nickel phosphides at overpotentials as low as 10 mV. *Energy Environ. Sci.* **2018,** *11*, 2550-2559; (b) A patent entitled "Hydrogenation of formic acid to formaldehyde claimed the electroreduction of CO_2 into formic acid, the hydrogenation of formic acid into formaldehyde and the Ca-catalyzed formose reaction as a pathway to a mixture of carbohydrates, see Masel R. I.; Ni Z. R.; Chen Q.; Rosen B. A. Hydrogenation of formic acid to formaldehyde. US 9,193,593 B2, 2015.

20. Zhang, D.; Jarava-Barrera, C.; Bontemps, S. Selective Reductive Dimerization of CO_2 into Glycolaldehyde. *ACS Catal.* **2021,** *11*, 4568-4575.

21. Béthegnies, A.; Escudié, Y.; Nuñez-Dallos, N.; Vendier, L.; Hurtado, J.; del Rosal, I.; Maron, L.; Bontemps, S. Reductive CO_2 Homocoupling: Synthesis of a Borylated C_3 Carbohydrate. *ChemCatChem* **2019,** *11*, 760-765.

22. (a) Das Neves Gomes, C.; Blondiaux, E.; Thuéry, P.; Cantat, T. Metal-Free Reduction of CO_2 with Hydroboranes: Two Efficient Pathways at Play for the Reduction of CO_2 to Methanol. *Chem. Eur. J.* **2014,** *20*, 7098-7106; (b) Cantat, T.; Gomes, C.; Blondiaux, E.; Jacquet, O. Method for preparing oxyborane compounds for subsequent hydrolysis to give methane derivatives. WO2014162266A1, 2014; (c) Jin, G.; Werncke, C. G.; Escudié, Y.; Sabo-Etienne, S.; Bontemps, S. Iron-Catalyzed Reduction of CO_2 into Methylene: Formation of C–N, C–O, and C–C Bonds. *J. Am. Chem. Soc.* **2015,** *137* 9563–9566.

23. Chakraborty, S.; Zhang, J.; Krause, J. A.; Guan, H. An Efficient Nickel Catalyst for the Reduction of Carbon Dioxide with a Borane. *J. Am. Chem. Soc.* **2010,** *132*, 8872-8873.

24. (a) Bontemps, S. Boron-Mediated Activation of Carbon Dioxide. *Coord. Chem. Rev.* **2016,** *308, Part 2*, 117-130; (b) Chong, C. C.; Kinjo, R. Catalytic Hydroboration of Carbonyl Derivatives, Imines, and Carbon Dioxide. *ACS Catal.* **2015,** *5*, 3238-3259.

25. (a) Huang, F.; Zhang, C.; Jiang, J.; Wang, Z.-X.; Guan, H. How Does the Nickel Pincer Complex Catalyze the Conversion of CO_2 to a Methanol Derivative? A Computational Mechanistic Study. *Inorg. Chem.* **2011,** *50*, 3816-3825; (b) Bontemps, S.; Sabo-Etienne, S. Trapping Formaldehyde in the Homogeneous Catalytic Reduction of Carbon Dioxide. *Angew. Chem. Int. Ed.* **2013,** *52*, 10253-10255; (c) Bontemps, S.; Vendier, L.; Sabo-Etienne, S. Borane-Mediated Carbon Dioxide Reduction at Ruthenium: Formation of C_1 and C_2 Compounds. *Angew. Chem. Int. Ed.* **2012,** *51*, 1671-1674; (d) Espinosa, M. R.; Charboneau, D. J.; Garcia de Oliveira, A.; Hazari, N. Controlling Selectivity in the Hydroboration of Carbon Dioxide to the Formic Acid, Formaldehyde, and Methanol Oxidation Levels. *ACS Catal.* **2018,** *9*, 301-314.

26. Bontemps, S.; Vendier, L.; Sabo-Etienne, S. Ruthenium-Catalyzed Reduction of Carbon Dioxide to Formaldehyde. *J. Am. Chem. Soc.* **2014,** *136*, 4419-4425.

27. Murphy, L. J.; Hollenhorst, H.; McDonald, R.; Ferguson, M.; Lumsden, M. D.; Turculet, L. Selective Ni-Catalyzed Hydroboration of CO_2 to the Formaldehyde Level Enabled by New PSiP Ligation. *Organometallics* **2017,** *36*, 3709-3720.

28. Desmons, S.; Zhang, D.; Mejia Fajardo, A.; Bontemps, S. Versatile CO_2 Transformations into Complex Products: A One-pot Two-step Strategy. *J. Vis. Exp.* **2019,** *153*, e60348.

29. Courtemanche, M.-A.; Pulis, A. P.; Rochette, E.; Legare, M.-A.; Stephan, D. W.; Fontaine, F.-G. Intramolecular B/N frustrated Lewis pairs and the hydrogenation of carbon dioxide. *Chem. Comm.* **2015,** *51*, 9797-9800.

30. Li, J.; Daniliuc, C. G.; Kehr, G.; Erker, G. Preparation of the Borane (Fmes)BH2 and its Utilization in the FLP Reduction of Carbon Monoxide and Carbon Dioxide. *Angew. Chem. Int. Ed.* **2019,** *58*, 6737-6741.

31. (a) Rauch, M.; Strater, Z.; Parkin, G. Selective Conversion of Carbon Dioxide to Formaldehyde via a Bis(silyl)acetal: Incorporation of Isotopically Labeled C_1 Moieties Derived from Carbon Dioxide into Organic Molecules. *J. Am. Chem. Soc.* **2019,** *141*, 17754-17762; (b) Frogneux, X.; Blondiaux, E.; Thuéry, P.; Cantat, T. Bridging Amines with CO_2: Organocatalyzed Reduction of CO_2 to Aminals. *ACS Catal.* **2015,** *5*, 3983-3987; (c) Zhang, Y.; Zhang, T.; Das, S. Catalytic transformation of CO_2 into C_1 chemicals using hydrosilanes as a reducing agent. *Green Chem.* **2020,** *22*, 1800-1820; (d) Li, W.-D.; Chen, J.; Zhu, D.-Y.; Xia, J.-B. Fe-Catalyzed Pictet-Spengler-Type Cyclization via Selective Four-Electron Reductive Functionalization of CO_2. *Chin. J. Chem.* **2021,** *39*, 614-620; (e) Zhao, Y.; Guo, X.; Ding, X.; Zhou, Z.; Li, M.; Feng, N.; Gao, B.; Lu, X.; Liu, Y.; You, J. Reductive CO_2 Fixation via the Selective Formation of C–C Bonds: Bridging Enaminones and Synthesis of 1,4-Dihydropyridines. *Org. Lett.* **2020,** *22*, 8326–8331; (f) Zhu, D.-Y.; Li, W.-D.; Yang, C.; Chen, J.; Xia, J.-B. Transition-Metal-Free Reductive Deoxygenative Olefination with CO_2. *Org. Lett.* **2018,** *20*, 3282-3285; (g) Zhu, D.-Y.; Fang, L.; Han, H.; Wang, Y.; Xia, J.-B. Reductive CO_2 Fixation via Tandem C–C and C–N Bond Formation: Synthesis of Spiro-indolepyrrolidines. *Org. Lett.* **2017,** *19*, 4259-4262.

32. (a) Hönig, M.; Sondermann, P.; Turner, N. J.; Carreira, E. M. Enantioselective Chemo- and Biocatalysis: Partners in Retrosynthesis. *Angew. Chem. Int. Ed.* **2017,** *56*, 8942–8973; (b) Schmidt, N. G.; Eger, E.; Kroutil, W. Building Bridges: Biocatalytic C–C-Bond Formation toward

Multifunctional Products. *ACS Catal.* **2016,** *6*, 4286-4311; (c) Müller, M. Recent Developments in Enzymatic Asymmetric C-C Bond Formation. *Adv. Synth. Catal.* **2012,** *354*, 3161-3174; (d) Prier, C. K.; Arnold, F. H. Chemomimetic Biocatalysis: Exploiting the Synthetic Potential of Cofactor-Dependent Enzymes To Create New Catalysts. *J. Am. Chem. Soc.* **2015,** *137*, 13992-14006.

33. (a) Schürmann, M.; Sprenger, G. A. Fructose-6-phosphate Aldolase Is a Novel Class I Aldolase from Escherichia coli and Is Related to a Novel Group of Bacterial Transaldolases. *J. Biol. Chem.* **2001,** *276*, 11055-11061; (b) Hernández, K.; Szekrenyi, A.; Clapés, P. Nucleophile Promiscuity of Natural and Engineered Aldolases. *ChemBioChem* **2018,** *19*, 1353-1358; (c) Clapés, P., Aldol Reactions. In *Biocatalysis in Organic Synthesis*, K. Faber, W.-D. F., N. J. Turner, Ed. Georg Thieme Verlag: Stuttgart, 2015; Vol. 2, pp 31-92.

34. Szekrenyi, A.; Garrabou, X.; Parella, T.; Joglar, J.; Bujons, J.; Clapés, P. Asymmetric Assembly of Aldose Carbohydrates from Formaldehyde and Glycolaldehyde by Tandem Biocatalytic Aldol Reactions. *Nat Chem* **2015,** *7*, 724-729.

35. (a) Siegel, J. B.; Smith, A. L.; Poust, S.; Wargacki, A. J.; Bar-Even, A.; Louw, C.; Shen, B. W.; Eiben, C. B.; Tran, H. M.; Noor, E.; Gallaher, J. L.; Bale, J.; Yoshikuni, Y.; Gelb, M. H.; Keasling, J. D.; Stoddard, B. L.; Lidstrom, M. E.; Baker, D. Computational Protein Design Enables a Novel one-Carbon Assimilation Pathway. *Proc. Natl. Acad. Sci.* **2015,** *112*, 3704-3709; (b) Poust, S.; Piety, J.; Bar-Even, A.; Louw, C.; Baker, D.; Keasling, J. D.; Siegel, J. B. Mechanistic Analysis of an Engineered Enzyme that Catalyzes the Formose Reaction. *ChemBioChem* **2015,** *16*, 1950-1954.

36. (a) Huang, X.; Cao, M.; Zhao, H. Integrating biocatalysis with chemocatalysis for selective transformations. *Curr. Opin. Chem. Biol.* **2020,** *55*, 161-170; (b) Denard, C. A.; Hartwig, J. F.; Zhao, H. Multistep One-Pot Reactions Combining Biocatalysts and Chemical Catalysts for Asymmetric Synthesis. *ACS Catal.* **2013,** *3*, 2856-2864.

37. Rudroff, F.; Mihovilovic, M. D.; Gröger, H.; Snajdrova, R.; Iding, H.; Bornscheuer, U. T. Opportunities and challenges for combining chemo- and biocatalysis. *Nat. Catal.* **2018,** *1*, 12-22.

38. A fifth BBA was obtained from CO_2, however, two reactions were necessary to conduct the hydroboration reactions with two different hydroboranes, see: Frick, M.; Horn, J.; Wadepohl, H.; Kaifer, E.; Himmel, H. J. Catalyst-Free Hydroboration of CO_2 With a Nucleophilic Diborane(4). *Chem. Eur. J.* **2018**, *24*, 16983-16986.

39. Chatterjee, T.; Boutin, E.; Robert, M. Manifesto for the routine use of NMR for the liquid product analysis of aqueous CO_2 reduction: from comprehensive chemical shift data to formaldehyde quantification in water. *Dalton Trans.* **2020,** *49*, 4257-4265.

40. In this case, formaldehyde could also be released in anhydrous conditions with the addition of CsF at room temperature.

41. Such condensation reaction are usually conducted under anhydrous conditions and drying agent. The long reaction time observed is explained by the presence of water and the absence of drying agent.

42. Magnusson, A. O.; Szekrenyi, A.; Joosten, H.-J.; Finnigan, J.; Charnock, S.; Fessner, W.-D. nanoDSF as screening tool for enzyme libraries and biotechnology development. *The FEBS Journal* **2019,** *286*, 184-204.

43. Janzen, E.; Müller, M.; Kolter-Jung, D.; Kneen, M. M.; McLeish, M. J.; Pohl, M. Characterization of benzaldehyde lyase from Pseudomonas fluorescens: A versatile enzyme for asymmetric C–C bond formation. *Bioorg. Chem.* **2006,** *34*, 345-361.

44. As for the other measurements, this result was obtained as triplicate, and the blank test without FLS led to 0% conversion. .

45. (a) This 80% conversion is a personal communication from one author based on their reported 68% isolated yield, see ref previous ref; (b) Castillo, J. A.; Guérard-Hélaine, C.; Gutiérrez, M.; Garrabou, X.; Sancelme, M.; Schürmann, M.; Inoue, T.; Hélaine, V.; Charmantray, F.; Gefflaut, T.; Hecquet, L.; Joglar, J.; Clapés, P.; Sprenger, G. A.; Lemaire, M. A Mutant D-Fructose-6-Phosphate Aldolase (Ala129Ser) with Improved Affinity towards Dihydroxyacetone for the Synthesis of Polyhydroxylated Compounds. *Adv. Synth. Catal.* **2010,** *352*, 1039-1046.

46. Yang, J.; Sun, S.; Men, Y.; Zeng, Y.; Zhu, Y.; Sun, Y.; Ma, Y. Transformation of Formaldehyde into Functional Sugars via Multi-Enzyme Stepwise Cascade Catalysis. *Catal. Sci. Technol.* **2017,** *7*, 3459-3463.

47. (a) Carly, F.; Steels, S.; Telek, S.; Vandermies, M.; Nicaud, J.-M.; Fickers, P. Identification and characterization of EYD1, encoding an erythritol dehydrogenase in Yarrowia lipolytica and its application to bioconvert erythritol into erythrulose. *Bioresour. Technol.* **2018,** *247*, 963-969; (b) Ciriminna, R.; Fidalgo, A.; Ilharco, L. M.; Pagliaro, M. Dihydroxyacetone: An Updated Insight into an Important Bioproduct. *ChemistryOpen* **2018,** *7*, 233-236.

48. Schwander, T.; Schada von Borzyskowski, L.; Burgener, S.; Cortina, N. S.; Erb, T. J. A synthetic pathway for the fixation of carbon dioxide in vitro. *Science* **2016,** *354*, 900-904.

49. (a) Baker, M. V.; Field, L. D. Molecular hydrogen complexes as intermediates in the synthesis of iron phosphine complexes; a reinvestigataion of the preparation of bis(diphosphine) chlorohydridoiron complexes. *J. Organomet. Chem.* **1988,** *354*, 351-356; (b) Whittlesey, M. K.; Mawby, R. J.; Osman, R.; Perutz, R. N.; Field, L. D.; Wilkinson, M. P.; George, M. W. Transient and matrix photochemistry of $Fe(dmpe)_2H_2$ (dmpe = $Me_2PCH_2CH_2Me_2$): dynamics of C-H and H-H activation. *J. Am. Chem. Soc.* **1993,** *115*, 8627-8637; (c) Dombray, T.; Werncke, C. G.; Jiang, S.; Grellier, M.; Vendier, L.; Bontemps, S.; Sortais, J.-B.; Sabo-Etienne, S.; Darcel, C. Iron-Catalyzed C–H Borylation of Arenes. *J. Am. Chem. Soc.* **2015,** *137*, 4062-4065.

50. (a) Hooz, J.; Akiyama, S.; Cedar, F. J.; Bennett, M. J.; Tuggle, R. M. Lithium dimesitylborohydride bis(dimethoxyethane). New crystalline reagent for stereoselective reduction of ketones. *J. Am. Chem. Soc.* **1974,** *96*, 274-276; (b) Entwistle, C. D.; Marder, T. B.; Smith, P. S.; Howard, J. A. K.; Fox, M. A.; Mason, S. A. Dimesitylborane monomer-dimer equilibrium in solution, and the solid-state structure of the dimer by single crystal neutron and X-ray diffraction. *J. Organomet. Chem.* **2003,** *680*, 165-172.

51. Weese, K. J.; Bartlett, R. A.; Murray, B. D.; Olmstead, M. M.; Power, P. R. Synthesis and spectroscopic and structural characterization of derivatives of the quasi-alkoxide ligand $[OBMes_2]^-$ (Mes = 2,4,6-$Me_3C_6H_2$). *Inorg. Chem.* **1987,** *26*, 2409-2413.

Insert Table of Contents artwork here

TOC: